1976AJ.....81..455J

THE ASTRONOMICAL JOURNAL VOLUME 81, NUMBER 6 JUNE 1976

Gravitational deflection of light: solar eclipse of 30 June 1973 II. Plate reductions

Burton F. Jones*
Royal Greenwich Observatory, Herstmonceux, Sussex, England
University of Texas, Austin, Texas 78712
(Received 21 July 1975; revised 3 February 1976)

The eclipse plates obtained on 30 June 1973 and the comparison plates obtained in November 1973 at Chinguetti, Mauritania, were measured on the Galaxy II comparator at the Royal Greenwich Observatory and with a PDS microphotometer at the University of Texas, Austin. A description of the reduction procedure is given and values are determined for probable errors. The final value obtained for the light deflection, extrapolated to the solar limb, is $L=(0.95\pm0.11$ std. dev.$)\,L_E$, where $L_E=1.75$ arcsec is the value predicted by general relativity theory.

I. GALAXY MEASUREMENT

THE preceding paper describes the Texas expedition and the various series of plates obtained during the eclipse and five months later with the identical equipment. In what follows, the *eclipse field* will refer to the star field which contained the Sun during the eclipse, and the *comparison field* the star field 10° to the south which was also photographed on each plate containing the eclipse field. *Eclipse epoch* plates will refer to plates of the eclipse or comparison field taken during the eclipse, and *nighttime* plates to plates of these fields taken at night five months later.

The three eclipse epoch plates and three sets of nighttime plates of the same fields (Table I) were measured on the GALAXY measuring engine (Walker 1971; Pratt 1971) at the Royal Greenwich Observatory. All AGK3 or SAO stars even marginally present were included for measurement. The magnitude limit was about 9 for the eclipse field (60-sec exposure) and 8 for the comparison field (30-sec exposure). One hundred fifty stars were measured on the eclipse field and 60 on the comparison field. In addition, the 625 grid points were measured on each plate. Each field was measured twice, and the grid once, in both direct and reverse orientation.

Standard programs developed at Greenwich were used to correct the measures for a zero-point drift during the measuring run, and to match the same star measured on different plates. The four measures of each star on each plate were then combined. From this combination, the repeatability of GALAXY was found to be less than $\frac{1}{2}$ μm, close to the limit of $\frac{1}{3}$ μm set by GALAXY'S 1-μm least readout.

II. PDS MEASURES

The eclipse field only on the eclipse epoch plates and one set of night plates (Nos. 8, 9, 10) were measured on the PDS microdensitometer at Austin (Wray and Benedict 1974). A 260×260-μm raster scan was made around each faint star, and one of 500×500 μm around each bright star. The machine scanned with an aperture of 10×10 μm. For the faint stars, the density was dumped every 4 μm with a 4-μm separation between scans. The dump and separation were 10 μm for the bright stars. Several stars of intermediate brightness were scanned with both raster sizes. About 160 stars were measured on each plate, and measurements were made of the step wedges. Figure 1 shows density plots of stars of various magnitudes, and illustrates the amount of noise present for faint stars.

A program developed by W. F. van Altena and modified by R. Abbot and myself was used to reduce the density arrays to x, y positions. The program finds the center of density (or intensity) (x_0, y_0) defined by

$$Z_0=\frac{\iint_{\text{raster}} ZW(x,y)D(x,y)\,dx\,dy}{\iint_{\text{raster}} W(x,y)D(x,y)\,dx\,dy} \quad (Z=x \text{ or } y), \quad (1)$$

where $D(x,y)$ is the density and $W(x,y)$ is a weighting function.

The basic requirements of the weighting function are that it should go to zero as the background noise becomes appreciable and that it should be constant along lines of constant density. If we assume a bivariate normal distribution for the density, which preliminary reductions showed to be reasonable, then curves of equal density will be ellipses given by

$$\frac{(x-x_0)^2}{\sigma_x^2}-\frac{2\rho(x-x_0)(y-y_0)}{\sigma_x\sigma_y}+\frac{(y-y_0)^2}{\sigma_y^2}=C^2, \quad (2)$$

where σ_x, σ_y are the dispersions and ρ the correlation coefficient (Trumpler and Weaver 1962). We require W to be a function of C. The following weighting scheme

* Now at Lick Observatory, University of California, Santa Cruz, California 95060.

© American Astronomical Society • Provided by the NASA Astrophysics Data System

1976AJ.....81..455J

TABLE I. Plates measured on GALAXY.

Plate	Plate holder	Date (1973)	Outside temp (°C)	Comment
46	2	30 June	38.3	Plates taken during eclipse, each containing the eclipse and comparison field.
47	3			
48	4			
8	2	13 Nov	16.9	Eclipse and comparison field taken with telescope at same temperature as eclipse plates.
9	3			
10	4			
18	1	16 Nov	18.9	Eclipse and comparison fields taken with telescope at nighttime temp. Telescope refocussed.
22	5			
23	6			
28	1	17 Nov	18.3	Eclipse and comparison fields taken with telescope at nighttime temp. Telescope refocussed.
29	2			
30	3			
31	4			
32	5			
33	6			

The eclipse field only on plates 8–10 and 46–48 was also measured on the PDS.

was adopted:

$$W(C)=\begin{cases}1, & C\leq 0.5\\ 1.25-0.5C, & 0.5\leq C\leq 2.5 \text{ in units of } \mu\text{m}\\ 0, & C>2.5.\end{cases} \quad (3)$$

This goes to zero as the density due to the star becomes comparable to the noise, and does not give the saturated central portion of the image undue weight.

The program initially sets $W=1$ for all x, y and calculates (x_0,y_0) using Eq. (1). It then calculates σ_x, σ_y, ρ, and using these values and Eqs. (2) and (3) to calculate W, recalculates (x_0,y_0). Depending on the brightness of the star, from one to five such iterations are necessary before (x_0,y_0) changes by less than 0.2 μm.

The step-wedge calibrations were used to transform the density into intensity units, and a reduction was carried out using intensity units instead of density. The rms difference in position between the intensity and density reductions was 0.3 μm and the mean difference was only 0.05 μm. The positions used for further reductions were those obtained from the density reductions.

The PDS was not nearly as stable as GALAXY. Several stars were monitored periodically during the course of measurement, and these show drifts of up to 3 μm.

In doing the reductions one obtains for each star the quantity

$$V=\int\int_{\text{raster}} W(x,y)D(x,y)\,dx\,dy, \quad (4)$$

which is a good measure of a star's brightness.

III. GRID REDUCTIONS AND EMULSION SHIFTS

The GALAXY measures of the grid points were used to check for emulsion shifts. The grid positions on all plates were reduced to the positions on plate 8 assuming the differences in position to be a general linear function of the coordinates. Average positions were formed for each grid point. The positions on each plate were then reduced to these average positions, and new average positions formed. The residuals from these reductions showed large-scale patterns. An example is illustrated in Fig. 2. Further investigation showed that terms in x^2 and xy were needed in the x reduction and xy and y^2 in the y reduction. Furthermore, the term in x^2 in x was the same as xy in y (within the errors), and the xy term in x the same as the y^2 term in y. This is what one expects if the plates were not pressed firmly to the master grid when the grid points were put on, and mimics a difference in tangent point in the reduction of star fields.

When reductions were done including these quadratic terms, the average unit weight error for a plate was 0.68 μm (dispersion 0.13 μm), and the residuals showed no large-scale patterns. We conclude that large-scale emulsion shifts are unimportant.

IV. CORRECTIONS FOR REFRACTION, ABERRATION, AND PROPER MOTION

The measured positions were corrected for proper motion, refraction, and aberration using a method and program developed by C. A. Murray and modified by myself (Murray, Tucker, and Clements 1971). Terms to third order in the zenith distance were used for the refraction corrections. The first-order refraction constant was computed individually for the temperature, pressure, and humidity at the epoch of each plate, and for a wavelength of 4400 Å, the center of our passband. The aberration correction took account of both annual and diurnal aberration, including the e terms.

SAO positions and proper motions were used to compute each star's true positions at the plate and eclipse epoch. Aberration and refraction corrections (Murray, Tucker, and Clements 1971) were then applied to the true positions at the plate epoch to give the apparent positions at the plate epoch. The difference between the true positions at the eclipse epoch and the apparent positions at the plate epoch, suitably transformed to the scale and orientation of the plate, are the corrections to be applied to the measured coordinates.

V. OUTLINE OF REDUCTION METHODS

Suppose we have a set of measurements of the eclipse field taken at eclipse time (x_i^e,y_i^e) and a set taken at night (x_i^n,y_i^n), both corrected to above the atmosphere and to a common epoch. We have determined the scale change and tangent point difference from a comparison field or by some other means, and have corrected the

© American Astronomical Society • Provided by the NASA Astrophysics Data System

1976AJ.....81..455J

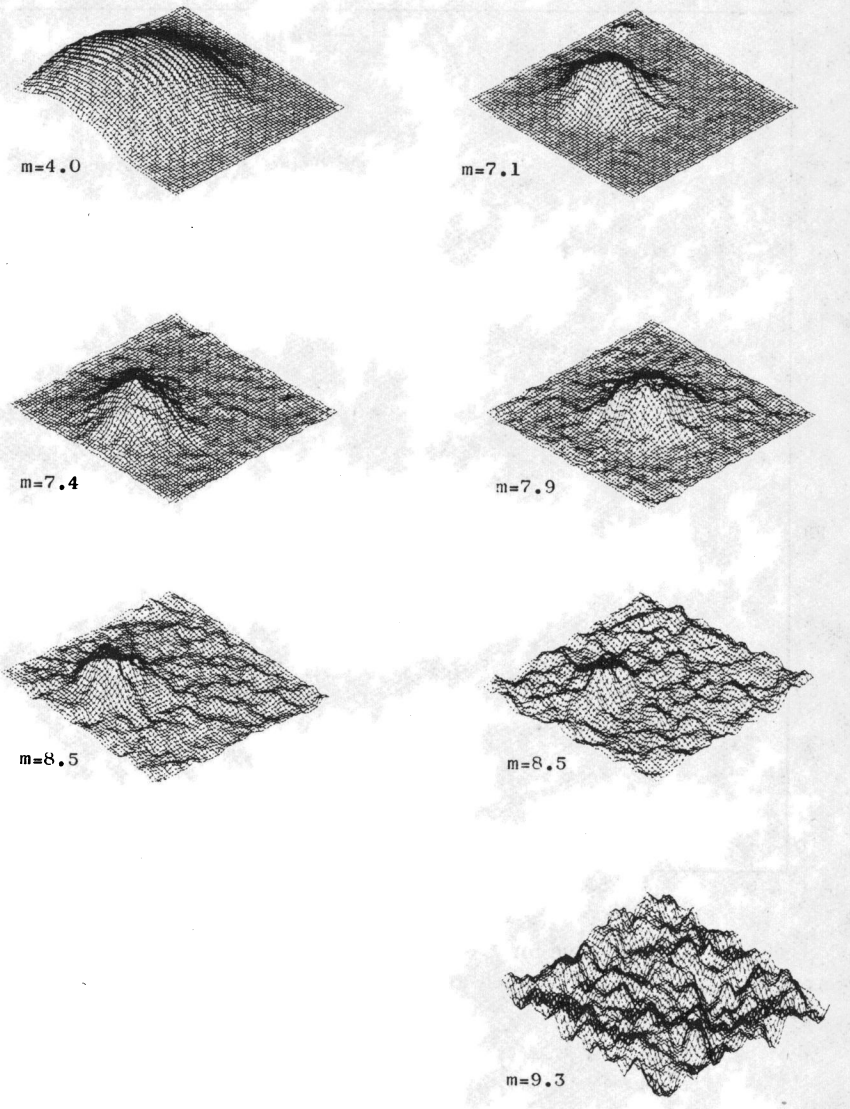

FIG. 1. Density plots of PDS measurements of stars of various magnitudes. Maximum density has been scaled to be the same for each star. Magnitudes are indicated.

eclipse measures for these effects. The differences between the two sets of measures will then be due to an orientation and zero-point shift, and the light deflection. That is

$$\Delta\mathbf{X}_i = \mathbf{D}_i\mathbf{L}, \tag{5}$$

where

$$\Delta\mathbf{X}_i = \begin{bmatrix} x_i^n - \cos\theta & x_i^e \\ y_i^n - \cos\theta & y_i^e \end{bmatrix},$$

$$\mathbf{D} = \begin{bmatrix} y_i^e & 1 & 0 & x_i^e/r_i^{-2} \\ -x_i^e & 0 & 1 & y_i^e/r_i^{-2} \end{bmatrix}, \tag{6}$$

$$\mathbf{L} = [B(=\sin\theta), C_x, C_y, L].$$

In Eq. (6), L is the light deflection, C_x, C_y are the zero-point shifts, θ is the rotation angle, and r_i is the distance from the Sun. We can use Eqs. (5) as equations of condition in a least-squares adjustment. The totality of equations of condition is

$$\Delta\mathbf{X} = \mathbf{D}\mathbf{L}, \tag{7}$$

where

$$\Delta\mathbf{X}^T = [\Delta\mathbf{X}_1{}^T, \Delta\mathbf{X}_2{}^T, \ldots, \Delta\mathbf{X}_n{}^T], \tag{8}$$
$$\mathbf{D}^T = [\mathbf{D}_1{}^T, \mathbf{D}_2{}^T, \ldots, \mathbf{D}_n{}^T].$$

The solution to the normal equations is then

$$\mathbf{L} = [\mathbf{D}^T\mathbf{D}]^{-1}[\mathbf{D}^T\Delta\mathbf{X}]. \tag{9}$$

These equations are nonlinear, since $\cos\theta$ appears in the $\Delta\mathbf{X}$ matrix. An iterative procedure must be used, initially setting $\theta=0$ in $\Delta\mathbf{X}$, solving Eq. (9) and using this value of θ in $\Delta\mathbf{X}$ for another iteration. One continues this process until $\cos\theta$ does not change by some small amount, for these reductions 10^{-8}.

© American Astronomical Society • Provided by the NASA Astrophysics Data System

1976AJ.....81..455J

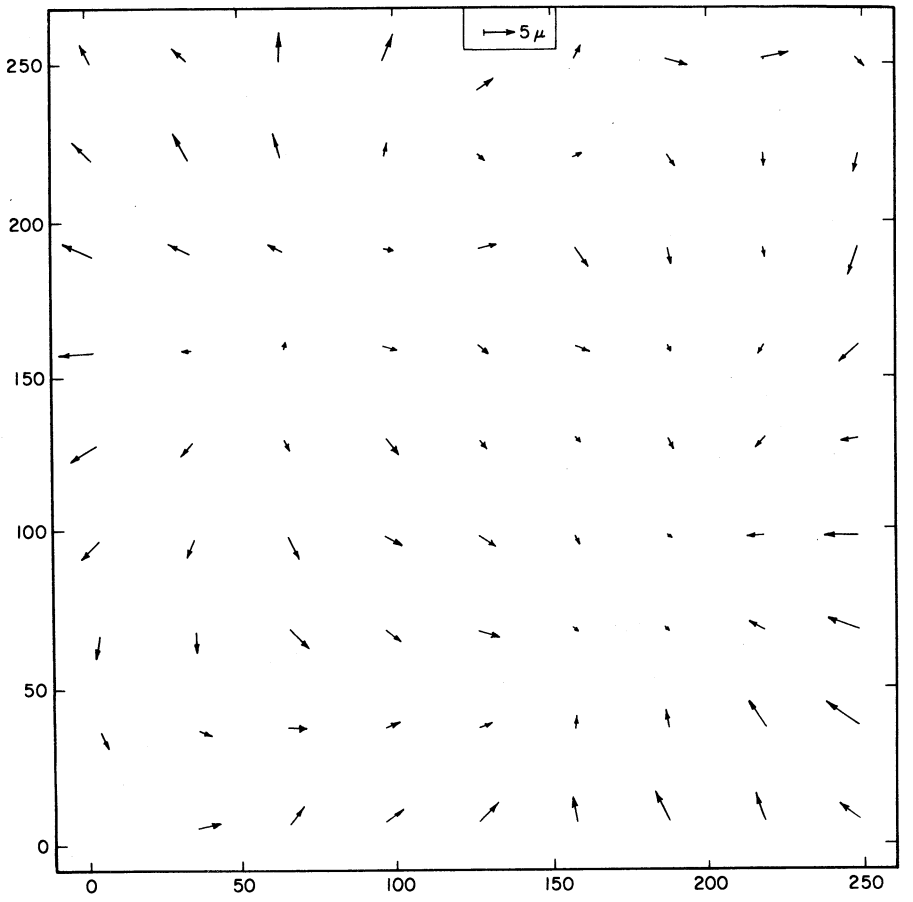

FIG. 2. Grid point residuals, Plate 85.

Using Eqs. (5) to solve for L one obtains a standard error for L given by (Freudlich and Ledermann 1944)

$$\sigma_{L1}=\sigma_0\left\{n\left[\frac{1}{h}-(\zeta^2+\eta^2)-\frac{(\bar{x}\eta-\bar{y}\zeta)^2}{a-\bar{x}^2-\bar{y}^2}\right]\right\}^{-\frac{1}{2}}, \quad (10)$$

where

$$n=\text{number of stars},$$

$$\frac{1}{h}=\frac{1}{n}\sum_{i=1}^{n}1/r_i^2, \quad a=\frac{1}{n}\sum_{i=1}^{n}r_i^2,$$

$$\bar{x}=\frac{1}{n}\sum_{i=1}^{n}x_i, \quad \bar{y}=\frac{1}{n}\sum_{i=1}^{n}y_i, \quad (11)$$

$$\zeta=\frac{1}{n}\sum_{i=1}^{n}\frac{x_i}{r_i^2}, \quad \eta=\frac{1}{r}\sum_{i=1}^{n}\frac{y_i}{r_i^2},$$

and σ_0 is the unit weight error of the solution. For a field with stars symmetric about the Sun, Eq. (10) simplifies to

$$\sigma_{L1}\approx\sigma_0\left(\frac{h}{n}\right)^{\frac{1}{2}}. \quad (12)$$

Suppose we attempted to solve for the light deflection and scale change in one solution, that is, we change Eqs. (6) to

$$\Delta\mathbf{X}_i=\begin{bmatrix}x_i^n-x_i^e\\ y_i^n-y_i^e\end{bmatrix},$$

$$\mathbf{D}_i=\begin{bmatrix}x_i^e & y_i^e & 1 & 0 & x_i^e r_i^{-2}\\ y_i^e & -x_i^e & 0 & 1 & y_i^e r_i^{-2}\end{bmatrix}, \quad (13)$$

$$\mathbf{L}^T=[A \quad B \quad Cx \quad Cy \quad L].$$

We would then get a mean error for L of (Freundlich and Ledermann 1944)

$$\sigma_{L2}=\sigma_0\left\{n\left[\frac{1}{h}-\frac{1}{a}-\frac{(a\zeta-\bar{x})^2+(a\eta-\bar{y})^2}{a(a-\bar{x}^2-\bar{y}^2)}\right]\right\} \quad (14)$$

which simplifies for a symmetric field to

$$\sigma_{L2}\approx\sigma_0\left[n\left(\frac{1}{h}-\frac{1}{a}\right)\right]^{-\frac{1}{2}}. \quad (15)$$

It is evident that the weight in general will be much reduced. In our case the error in L would be increased by about 50%.

© American Astronomical Society • Provided by the NASA Astrophysics Data System

1976AJ.....81..455J

However, if we use Eqs. (6) to solve for L, we are correcting the eclipse measures by some scale change determined from the comparison field. Because of the correlation between the scale change and the light deflection, a difference ΔS between two values of the adopted scale change will lead to a difference ΔL between the calculated light deflections of (Freundlich and Ledermann 1944)

$$\Delta L = -h\left[\frac{1-(\bar{x}\zeta+\bar{y}\eta)}{1-h(\zeta^2+\eta^2)-h(\bar{x}\zeta-\bar{y}\eta)/(a-\bar{x}^2-\bar{y}^2)}\right]\Delta S = -\xi\Delta S. \tag{16}$$

The scale change computed from the comparison field will have some mean error σ_s associated with it, and this, from Eq. (16), will introduce an error in L of

$$\sigma_{L3} = \xi\sigma_s, \tag{17}$$

which for a symmetric field reduces to

$$\Delta L \approx -h\Delta S, \quad \sigma_{L3} \approx h\sigma_s. \tag{18}$$

Equations (16)–(18) were derived assuming that the tangent points are known from some source other than the comparison field, and are known without error. However, for a symmetric field, it is easy to show, by the same method Freundlich and Ledermann used in deriving Eq. (16), that there is no correlation between small errors in the tangent point derived from a comparison field and either the light deflection or the scale change. Thus, Eqs. (18) remain valid even if the tangent point is determined using the comparison field. Both σ_{L1} and σ_{L3} depend on the size of our field. The exact form of the dependence is determined by the distribution of stars in the field, but for uniform star field, density ρ stars per unit area, we would have approximately

$$n \approx \int_1^R 2\pi\rho r\, dr = \pi\rho(R^2-1),$$
$$\frac{1}{h} \approx \frac{1}{n}\int_1^R \frac{2\pi\rho r\, dr}{r^2} = \frac{2\ln R}{R^2-1}, \tag{19}$$
$$a \approx \frac{1}{n}\int_1^R 2\pi r^3\, dr = \tfrac{1}{2}(R^2+1),$$

where the integrations are carried out from the limb of the Sun to some arbitrary distance R. For large R we then have

$$\sigma_{L1} \propto \sigma_0(\ln R)^{-\frac{1}{2}}, \quad \sigma_{L3} \propto \sigma_s\frac{R^2}{\ln R}. \tag{20}$$

σ_{L1} decreases and σ_{L3} increases with R. If an *independent* scale determination and Eqs. (6) are used to determine L, the mean error in L will be $\sigma = (\sigma_{L1}^2+\sigma_{L3}^2)^{\frac{1}{2}}$. σ is a function of R, and will be a minimum at some limiting distance R_0. The inclusion of stars beyond R_0 in calculating the light deflection will lead to systematically wrong results for the light deflection.

VI. WEIGHTING

From preliminary reductions, it was obvious that the faint stars had much lower weight than the bright stars. As an illustration, Fig. 3 shows a plot of the total residual versus PDS magnitude for a reduction of plate 8 against plate 46. The following weighting scheme with the weight a function of magnitude was found to be adequate:

$$W(m) = \begin{cases} 1, & m \le m_0 \\ [\alpha m + (1-\alpha m_0)]^{-2}, & m > m_0. \end{cases} \tag{21}$$

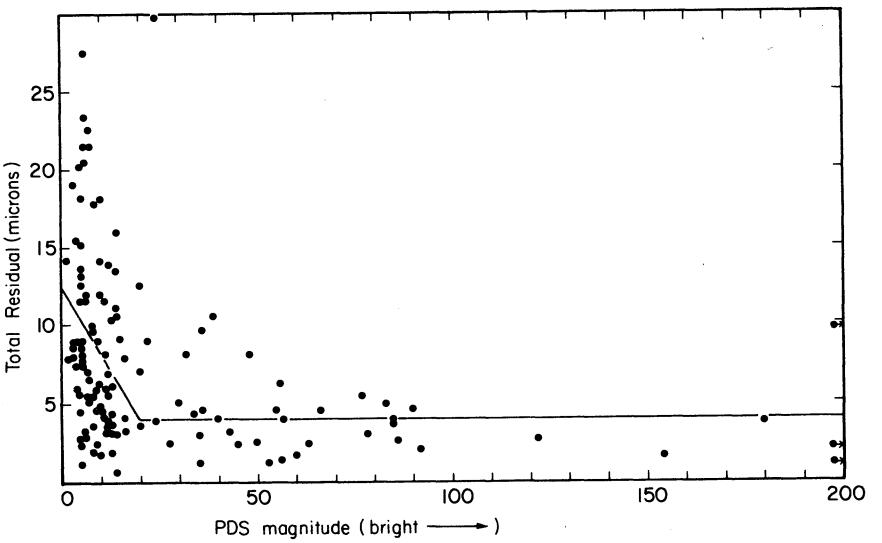

FIG. 3. Plot of total residual in micrometers versus PDS magnitude for reduction of plate 8 against plate 46, using PDS measures. $m_0 = 20$.

© American Astronomical Society • Provided by the NASA Astrophysics Data System

1976AJ.....81..455J

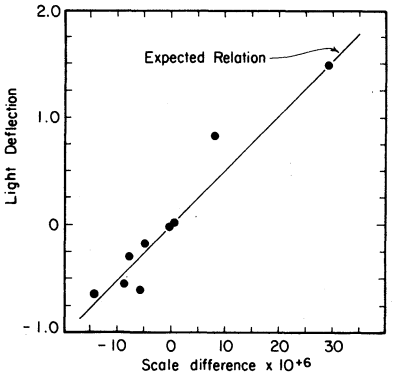

FIG. 4. Relation between difference in scale values between eclipse and comparison fields and light deflection for nighttime plates.

Plots like Fig. 3 were made for all plate combinations of interest and m_0 and α were determined by inspection. Solutions obtained using this weighting scheme showed no dependence of the weighted residuals on the weight or magnitude, indicating that the scheme is satisfactory. These weights were used in all subsequent reductions.

VII. SCALE PROBLEMS

To investigate scale changes, the *nighttime* plates were reduced against each other in pairs. Two reductions were done for each plate pair, first using the comparison field to determine the scale change and tangent points, and the eclipse field and Eqs. (5) to determine a light deflection, and then reversing the roles of the eclipse and comparison fields. Within the errors, one expects the scale changes to be the same for the eclipse and comparison field, and the light deflection to be zero. This was not the case. Large differences in the scale between plates taken successively were found, and the scale changes were not the same for the eclipse and comparison field. For example, the scale change between plates 8 and 9, taken within seconds of each other, is 1.7×10^{-4} for the comparison field and 1.5×10^{-4} for the eclipse field, with mean errors of about 4×10^{-6}. Not only is this far too large to be accounted for by temperature or refraction changes between the two plates, but the difference in scale change between the eclipse and comparison field, 2×10^{-5}, is disturbingly large.

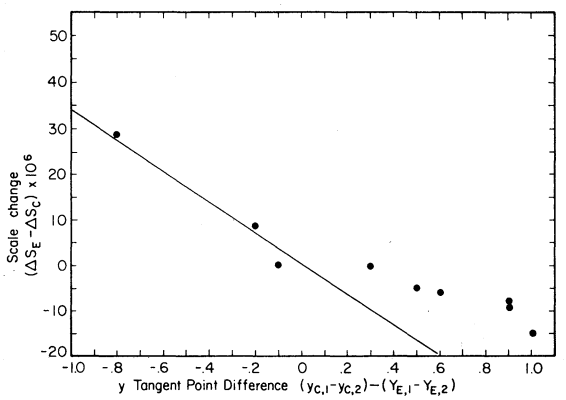

FIG. 5. Relationship between difference in scale change between eclipse and comparison field on same night-plate pair and the difference in tangent point difference.

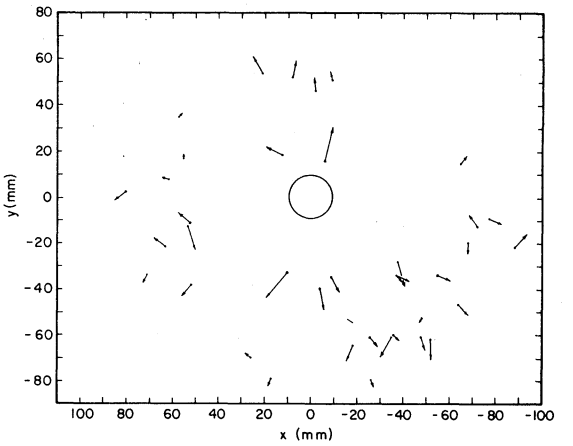

FIG. 6. Light deflections.

Because of the correlation between the scale change and the light deflection, the differences in the scale change between the comparison and eclipse exposures give rise to large spurious light deflections. Figure 4 shows a plot of the difference in scale change between the two fields on several plate pairs plotted against the light deflection from the eclipse field, with the relation from Eq. (16) plotted as a solid line. Figure 5 shows the scale change difference plotted against the y tangent point differences. The correlation shown in Fig. 6 between the scale change and tangent points indicates a tilting of the plate between the exposures of the eclipse and comparison fields. This is most easily explained by assuming that the springs that press the plates to the four studs on the back of the telescope were not strong enough. The solid line in Fig. 5 is the expected relationship under a simple model in which the plate pivots around two studs.

Because of this problem, it is impossible to use the comparison field to determine the scale change.

VIII. FINAL REDUCTIONS AND RESULTS

Because of the problems outlined in Sec. VII, we must use the eclipse field to calculate both the scale change and the light deflection.

A. Calculation of Average Positions

Average positions were obtained for each star in the eclipse field from the eclipse epoch plates, and separately for each set of nighttime plates. First, the positions on each plate of a series were reduced in a least-squares adjustment to the scale, orientation, and tangent point of the first plate of the series. Stars with weighted residuals greater than three times the unit weight error were rejected. The solutions were repeated until no stars were rejected. This usually took one to

© American Astronomical Society • Provided by the NASA Astrophysics Data System

1976AJ.....81..455J

two iterations. Average positions were then formed for each star. Next, these reductions were repeated, but this time reducing the positions on each plate of a series against the just found average positions, obtaining a new set of average positions. The second set of average positions did not differ significantly from the first set, and the process was stopped after one iteration.

These reductions gave sets of average positions obtained from each of the three series of night plates, and from the plates taken during the eclipse, each set of positions corrected to zero observer velocity, above the atmosphere, and to the eclipse epoch.

B. Scale and Tangent Point Determination

To determine the scale and tangent point differences between the eclipse positions and the positions from a set of nighttime plates, stars with $R \geq 10\ R_\odot$ were used. The average positions of these stars obtained from the eclipse plates were corrected for an assumed deflection of 1".75 (the Einstein value), and a least-squares adjustment performed to match the corrected average eclipse positions against each set of nighttime positions. An iterative procedure was used, rejecting stars with weighted residuals greater than three times the unit weight error, until solutions were obtained from which no stars were rejected. This usually took one to two iterations, and typically three out of 60 stars would be rejected.

The reason for using stars with $R \geq 10\ R_\odot$ in these reductions is that any error in the adopted light deflection used to correct the eclipse time measures gives rise to a scale error given approximately by Eq. (18) (since our field is nearly symmetric). The closer to the Sun we pick our stars, the larger the error from this source becomes. Without knowing the error in our adopted light deflection, we cannot pick the optimum value of the limiting radius, but our choice of 10 $R_\odot$ is such that an error of 10% in the adopted light deflection will give rise to an error of 0.05 arcsec in the final computed deflection (next section). Inclusion of stars with $R \leq 10\ R_\odot$ does not significantly increase the weight of the scale change determined from the least-squares adjustment.

TABLE II. Solution of daytime plates against mean positions from plates 8–10 for different values of limiting radius.

Limiting radius (unit $R_\odot$)	Number of stars	L	σ_{sol} (arcsec)	σ_{L3}	σ_T	Sym
5	6	1.71	0.29	0.05	0.29	0.04
6	14	1.74	0.23	0.06	0.24	0.01
7	19	1.73	0.19	0.08	0.21	0.01
8	31	1.63	0.17	0.09	0.19	0.03
9	39	1.66	0.15	0.10	0.18	0.05
10	51	1.64	0.15	0.12	0.19	0.04

L is the light deflection. σ_{sol} is the mean error in L from the least-squares adjustment [identical to Eq. (10)]. σ_{L3} is the error due to the error in the scale determination [Eq. (17)]. The mean error of the scale determination was 3.4×10^{-6}. $\sigma_T = (\sigma_{sol}^2+\sigma_{L3}^2)^{\frac{1}{2}}$. Sym is the fractional decrease in weight due to asymmetry.

TABLE III. Solutions of different nighttime mean measures against eclipse time measures. The same limiting radius of 7.5 $R_\odot$ is used in each case.

Plates (night)	Scale determination error$\times10^{-6}$	L (arcsec)	Number of stars
(8–10)	3.4	1.64±0.18	29
(22, 23)	2.9	1.89±0.18	30
(28–33)	3.4	1.63±0.20	29
PDS (8–10)	3.4	1.49±0.20	37

The error in L is the mean error from the solution.

C. Light Deflection Calculation

The eclipse epoch positions were corrected for each scale change and tangent point determination obtained in the last section, and Eqs. (5) and (9) were used to determine the light deflection, matching the eclipse epoch positions against each set of nighttime positions, for various values of the limiting radius.

Table II gives the results for the reduction against the positions obtained from plates 8–10, taken with the telescope unchanged from June. Solutions are given for various values of the limiting radius. Also listed are the mean error in L from the least-squares adjustment [identical to Eq. (10)], and the error in L due to the error in the scale determination, obtained in the last section, and the effect of the asymmetry of the star field.

Because the set of plates 8–10 were taken with the telescope unchanged from June, reductions using these plates should have the least chance of undetected systematic error. Moreover, because of drifts in the PDS measures and trouble with the ways on the PDS, the GALAXY measures are probably morer eliable. Table III gives results for the other nighttime plates as well as for the PDS measures.

D. Sources of Systematic Error

To check on refraction as an error source, solutions were run with the refraction set the same for all exposures, regardless of temperature and pressure. These

TABLE IV. Solutions of nighttime plates against each other. Limiting radius of 7.5 $R_\odot$. The error is the mean error from the least-squares adjustment.

Plates	Scale error	L (arcsec)	Number of stars
(8–10) (22–23)	2.9×10^{-6}	0.15±0.09	26
(8–10) (28–33)	2.9×10^{-6}	−0.07±0.10	26

© American Astronomical Society • Provided by the NASA Astrophysics Data System

1976AJ.....81..455J

TABLE V. Residuals and deflections from final solution.

SAO number	X	Y	M	R_x	R_y	D_x	D_y	D_r	Weight	Dis
78418	−80.765	−21.314	251	1.8	−4.2	−3.6	3.7	2.5	0.15	8.9
78430	−77.149	− 9.753	277	1.5	0.9	−3.5	−1.2	3.6	0.18	8.3
78437	−72.162	−12.162	239	−4.1	−3.2	2.0	2.8	−2.5	0.14	7.8
78445	−68.467	−20.642	687	−2.1	0.8	0.0	−1.5	0.4	1.00	7.6
78452	−65.328	14.931	384	−0.9	−1.3	−1.3	1.8	1.7	0.43	7.1
78460	−64.045	−47.290	357	1.0	0.9	−2.6	−2.1	3.3	0.33	8.5
78467	−55.227	−33.777	626	1.5	−0.5	−3.6	0.8	3.5	1.00	6.9
78471	−52.075	−60.464	311	−1.4	4.5	0.2	−6.0	4.4	0.22	8.5
78481	−48.175	−61.093	362	−0.5	2.0	−0.8	−3.6	3.3	0.35	8.3
78482	−47.985	−53.124	349	−2.0	−2.2	0.6	0.5	−0.8	0.31	7.6
78503	−38.824	−28.497	309	−0.8	4.2	−1.8	−6.2	5.1	0.22	5.1
78507	−38.070	−36.479	495	−1.1	−0.6	−1.1	−1.5	1.8	1.00	5.6
78508	−37.589	−36.254	588	1.6	−0.2	−3.8	−1.9	4.0	1.00	5.5
78510	−36.029	−60.703	376	0.4	−0.7	−1.5	−1.2	1.8	0.39	7.5
78514	−35.082	−61.276	246	−4.5	3.5	3.4	−5.4	3.1	0.14	7.5
78529	−26.823	−61.303	480	1.0	0.0	−1.9	−2.2	2.7	1.00	7.1
78534	−25.700	−80.722	391	0.0	−0.7	−0.5	−1.1	1.2	0.47	9.0
78542	−18.665	−65.785	337	−2.7	1.6	2.1	−3.8	3.1	0.28	7.3
78546	−16.001	−53.462	303	0.9	−1.9	−1.7	−0.7	1.2	0.21	5.9
78558	− 9.593	−35.685	524	0.4	−0.7	−1.4	−3.4	3.6	1.00	3.9
78557	− 9.134	51.883	768	−0.9	0.4	0.4	2.5	2.4	1.00	5.6
78568	− 5.990	16.490	231	−1.2	−1.2	−1.9	9.5	9.6	0.13	1.9
78572	− 2.156	46.803	683	−0.5	−0.3	0.4	3.6	3.5	1.00	5.0
78586	3.663	−40.004	655	1.2	1.7	−0.9	5.5	5.4	1.00	4.3
78596	7.737	52.084	691	0.9	−1.7	−0.5	4.7	4.6	1.00	5.6
78604	10.221	−33.186	356	−4.9	2.3	6.2	6.6	8.2	0.33	3.7
78610	12.215	18.864	331	−0.8	4.4	4.5	1.5	3.7	0.26	2.4
78626	17.036	−79.207	362	−0.5	0.3	0.9	2.2	2.3	0.35	8.6
78634	21.363	54.072	349	−1.9	−2.3	2.9	4.8	5.6	0.31	6.2
78646	26.181	−70.356	247	−0.6	−2.9	1.3	1.0	−0.5	0.15	8.0
78696	52.176	−11.120	684	−0.3	−3.3	3.2	2.7	2.5	1.00	5.7
78697	52.195	−39.943	319	−0.9	0.6	2.8	−2.1	3.4	0.24	7.0
78702	53.194	−12.831	253	4.8	6.1	−2.0	−6.7	−0.4	0.15	5.8
78707	55.728	17.906	347	2.6	−0.1	0.0	0.9	0.3	0.30	6.2
78712	57.534	35.161	372	1.8	0.4	0.2	0.8	0.6	0.38	7.2
78717	62.248	8.067	592	1.7	0.1	0.8	0.2	0.8	1.00	6.7
78722	63.773	−20.665	181	−0.7	−3.0	2.9	2.3	2.1	0.10	7.1
78742	71.208	−34.045	412	0.6	1.7	1.2	−2.5	2.1	0.59	8.4
78758	79.786	2.941	365	−1.1	2.4	3.1	−2.3	3.0	0.36	8.5

x and y coordinates are in millimeters, R_x, R_y are solution residuals in x and y in micrometers. D_x, D_y, and D_r are eclipse time deflections in micrometers in x, y and distance from Sun. Dis is the distance from the Sun in solar radii.

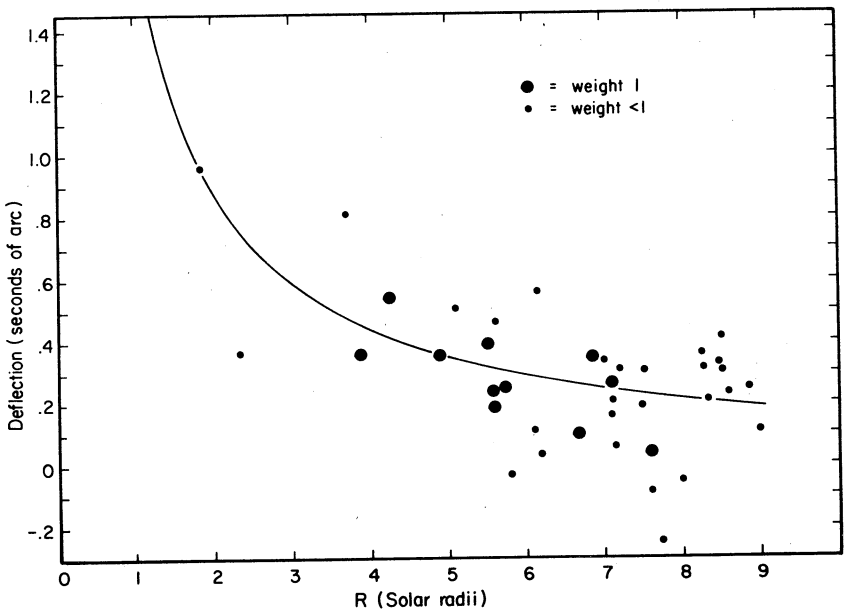

FIG. 7. Deflection versus distance.

© American Astronomical Society • Provided by the NASA Astrophysics Data System

1976AJ.....81..455J

reductions gave negligible differences from the other solutions.

Inspection of the images on the plates showed no traces of coma. Plots of solution residuals against $x(m-\bar{m})$ and $y(m-\bar{m})$ show no coma effects.

Because colors are not available for most of the stars, one cannot check color magnification effects [terms of the type $x(B-V)$, $y(B-V)$], but these terms should be absent, since we are doing differential reductions. Similarly, radial distortion (terms in xr^2, yr^2) should be small or absent, since the plates had nearly the same centers, and the telescope was unchanged between sets of plates. Investigation showed no radial distortion effects.

We can also check on systematic error by reducing the sets of night plates against each other. In this case we know the light deflection must be zero. Table IV gives the results of such reductions. These indicate small systematic errors, since the light deflections are nearly zero within the error.

E. Final Result

From the discussion of the last section, it would appear that the fifth solution (Line $R=9$) of Table II is our most reliable solution. Thus, our final result is $L=1.66\pm0.18$ arcsec. The error does not take into account a possible wrong choice of the light deflection in determining the scale change. Table V gives the residuals and the individual deflections for each star of this solution, and Figs. 6 and 7 show the results graphically.

ACKNOWLEDGMENTS

In addition to those thanked in Paper I, the staff of the astrometric department and computer section at the Royal Greenwich Observatory helped greatly with the measurements on GALAXY. Vassiliki Tsikoudi and Fritz Benedict gave much time and help in measuring the plates on the PDS. Richard Abbot gave valuable help in reducing the PDS measurements, and Gerry Grupsmith did the reductions of the grid measurements.

REFERENCES

Freundlich, E. F., and Ledermann, W. (1944). Mon. Not. R. Astron. Soc. **104**, 40.
Murray, C. A., Tucker, R. H., and Clements, E. D. (1971). R. Obs. Bull. **162**, 215.
Pratt, N. M. (1971). Publ. R. Obs. Edinburgh **8**, 103.
Trumpler, R. J., and Weaver, H. F. (1962). *Statistical Astronomy* (Dover, New York), p. 46.
Walker, G. S. (1971). Publ. R. Obs. Edinburgh **8**, 106.
Wray, J. D., and Benedict, G. F. (1974). Proc. Soc. Photo-Opt. Instrum. Eng. **44**, 137.

© American Astronomical Society • Provided by the NASA Astrophysics Data System